Theoretical studies on the electronic structure and spectral properties of versatile diarylethene-containing 1,10-phenanthroline ligands and their rhenium(I) complexes

Li-Li Shi, Yi Liao, Liang Zhao, Zhong-Min Su *, Yu-He Kan, Guo-Chun Yang, Shuang-Yang Yang

Institute of Functional Material Chemistry, Faculty of Chemistry, Northeast Normal University, Changchun 130024, People's Republic of China

Abstract

The structures of versatile diarylethene-containing 1,10-phenanthroline ligands (L_1 and L_2) and their rhenium(I) complexes $[Re(CO)_3(L)Cl]$ (**1** and **2**) in the ground and low-lying excited states have been optimized at the B3LYP functional and the ab initio configuration interaction singlets (CIS) level, respectively. The spectral properties are predicted with use of time-dependent density functional theory (TDDFT). As shown, the transition character of the strongest absorption band and luminescent spectrum for closed-ring complex **1** is different from that of **2**, the former has $\pi\pi^*$ character and the latter has MLCT and LLCT character. We presume the second triplet excited state contributes to the phosphorescence of **1**, while the lowest triplet excited state accounts for the phosphorescence of **2**. Spin–orbit coupling influences the excitation energies for d(Re)-joined transitions whereas it has negligible effect on the transition character for complexes **1** and **2**.
© 2007 Elsevier B.V. All rights reserved.

Keywords: Rhenium(I) complexes; B3LYP; CIS; TDDFT; Spectral properties

1. Introduction

Recently, there has been great interest in photochromic materials due to their potential application to optoelectronic devices, such as optical memories and optical switches [1]. Photochromic materials are the reversible transformation of a chemical species between two forms with different structures by photoirradiation [2], which change their absorption spectra drastically and reversibly. Besides the color change which is the origin of the term "photochromism", considerable research efforts are directed towards the changing of additional chemical and physical properties associated with this phenomenon. Although one of such important properties is the luminescence nature which is completely controlled by the photochromic interconversion [3], only a few examples have appeared to date [4].

Dithienylethene derivatives have received attention as promising photochromic materials due to thermal stability and excellent fatigue-resistant properties [1d,5]. Although there are many reports on dithienylethene derivatives, studies on the exploitation of these diarylethenes as ligands to form metal complexes are extremely rare. The combination of the diarylethene ligands and metal complex systems exhibits novel properties. Yam et al. [6] have reported their excellent work on this type of photochromic molecules, versatile diarylethene-containing 1,10-phenanthroline ligands and their rhenium(I) complexes $[Re(CO)_3(L)Cl]$ and found an interesting phenomenon: the difference between closed- and open-ring greatly influences the spectral properties, especially the luminescent property. It is well known that theoretical investigations on excited states are uncommon but necessary for exploring luminescent

behavior, because the calculation of excited-state properties typically requires significantly more computational effort than is needed for the ground states.

In this work, we take this diarylethene-containing 1,10-phenanthroline ligands (L_1 and L_2) and their rhenium(I) complexes $[Re(CO)_3(L)Cl]$ (**1** and **2**) for example to deeply investigate how the closed- and open-ring structures and the coordination of Re influence electronic and spectral properties. Then meaningful theoretical guidance can be obtained for synthesizing and designing novel photochromic materials with practical application perspective.

2. Computation methods

Calculations on the ground states of our title systems were carried out using DFT B3LYP [7]. 6-31G* basis set was employed on atoms C, H, S, N, Cl, O and "Double-ξ" quality basis set LANL2DZ was used on atom Re. A relativistic effective core potential (ECP) on Re replaced the inner core electrons leaving the outer core $[(5s^2) (5p^6)]$ electrons and the $(5d^6)$ valence electrons of Re(I). The excited-state geometry optimizations were performed at the level of configuration interaction considering single electron excitations (CIS) [8] from filled to unfilled molecular orbitals using the optimized ground-state geometry.

On the basis of ground- and excited-state geometries, TD-DFT approach [9] (Gaussian03 [10]) was applied to investigate the excited state electronic properties. This method is based on the Kohn–Sham formulation of DFT and uses the eigenvalues and eigenvectors of the Kohn–Sham equation. However, no spin–orbit interactions are included within this formulation. Recently, Wang and Ziegler [11] proposed a TDDFT formalism within the two-component relativistic zeroth-order regular approximation scheme based on the non-collinear exchange-correlation XC functional. This formalism can deal with spin–orbit coupling (SOC) and recover the threefold degeneracy of triplet excitations. To gain quantitative and qualitative insight into the effects of SOC on the excited states of heavy transition metal complexes (**1** and **2**), the two-component TDDFT formalism implemented in ADF 2006.01 program package [12] were performed at the ground states geometries obtained above with LB94 potential as the XC functional and the adiabatic local density approximation (ALDA) as the XC kernel. The electronic configurations of the molecular systems were described by a triple-ξ-plus-polarization (TZP) basis set, featuring Slater-type orbitals, for all atoms.

The geometries were fully optimized without symmetry constrains. AOMIX program package [13] was used in orbital composition analysis and charge decomposition analysis.

3. Results and discussion

The ligands and complexes in their closed-ring forms (L_1 and **1**) and open-ring forms (L_2 and **2**) are shown in Fig. 1. The electronic structures for the calculated
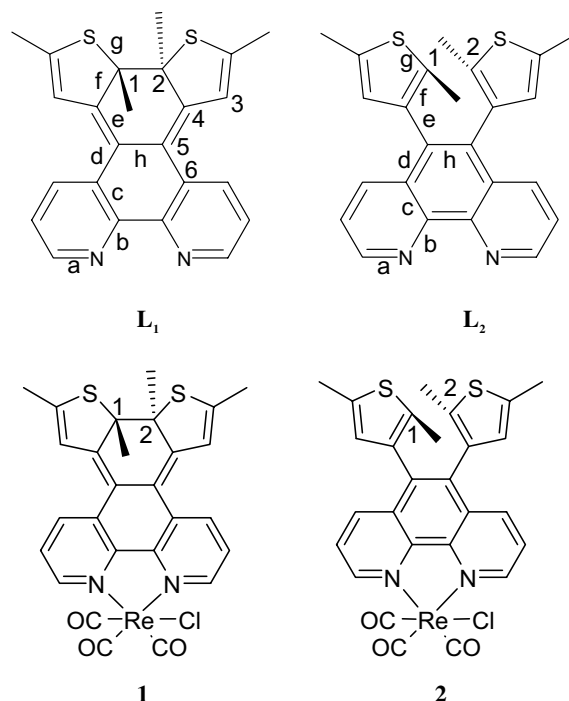

Fig. 1. Schematic structures of two ligands and two complexes in their open- and closed-ring forms.

ground-state geometries are examined in terms of the highest occupied and the lowest virtual molecular orbitals. The nature of the low-lying excited states is then explored using the TDDFT approach to derive both absorption and emission spectra, which are compared with available spectral data [6].

3.1. Molecular structure

There's no symmetrical constraint for the ligands during the geometry optimization, but according to the results we can approximately consider they possess C_2 symmetry. The selected bond lengths are summarized in Table 1. Compared with experimental data [6], the deviations of bond lengths are mostly between 0 and 0.02 Å, therefore this method are reliable for generating geometry configuration.

Table 1
Selected calculated bond lengths of the two ligands (Å)

Bond length	L_1	L_2
a	1.330	1.322(1.323)
b	1.343	1.353(1.353)
c	1.419	1.423(1.418)
d	1.474	1.450(1.448)
e	1.371	1.493(1.494)
f	1.537	1.374(1.365)
g	1.881	1.751(1.727)
h	1.483	1.379(1.363)

The experimental data are listed in parentheses.

Compared with L_2, the bonds closer to the two active centers (C_1 and C_2) of L_1 change more evidently (the most remarkable one is bond f ($f_1 = 1.54$ Å, $f_2 = 1.38$ Å, $\Delta f = 0.16$ Å)) owing to the redistribution of double bonds and the structure distortion which originates from the steric congestion of the methyl groups.

It is expected that L_1 should be in a planar. However, the calculated results reveal that the dihedral of 3–4–5–6 is 9.11°. Meanwhile, the coordination of Re makes this dihedral decreased to 7.81°. It follows that the coordination of Re diminishes the distortion degree of ligand section.

For the two complexes, Re(I) in each case exists in a distorted octahedral coordination structure. The alteration of calculated bond parameters between the open-ring and closed-ring forms mainly occurs in the ligands section. The changing trend is basically similar to that of ligands L_1 and L_2. Moreover, the bond lengths of Re–CO, Re–N and Re–Cl are approximately consistent with the reports from other groups [14].

Different structures due to photochromic interconversion will make the orbital character different, which will be discussed in the following section.

3.2. Molecular orbitals

Frontier molecular orbitals (FMO) play an important role in electronic excitations and transition characters. In order to express clearly the effect of closed–open ring and the coordination of Re on the distribution of orbitals, the highest five occupied and the lowest five virtual orbitals were plotted in Fig. 2 according to their energies (see Supporting information Table S1). Assignment of the character of each MO is made on the basis of its compositions expressed in terms of 1,10-phenanthroline ring (L_P), thiophene rings (L_T), Re central atom, Cl, CO ligands.

For L_1, the energy of HOMO is higher and the energy of LUMO is lower than that of L_2 due to its longer expanded π-conjugated network, making the energy gap of L_1 decreased. Compared with the corresponding orbitals of ligands, the coordination of Re(I) with electron-withdrawing properties causes a decrease in the energies of occupied and virtual MOs. Simultaneously, Re/Cl-localized orbitals are inserted into occupied MOs. Moreover, the components of HOMO and LUMO for L_1 and **1** are similar (see Fig. 3), which should account for the similarity on their spectral properties.

3.3. Metal–ligand interaction

To explore the effect of closed–open ring on metal(Re)–ligand(L) interaction, energy decomposition analysis (EDA) based on the work of Morokuma [15] and the ETS partitioning scheme of Ziegler [16] was carried out using ADF program at the level of BP86/TZP, and charge decomposition analysis (CDA) introduced by Frenking and coworkers [17] was performed at the level of B3LYP.

The bond dissociation energy is partitioned into ΔE_{prep} (the energy necessary to promote the two fragments from their equilibrium geometry and electronic ground state in the compound) and ΔE_{int} (the instantaneous interaction energy between the two fragments in the molecule). ΔE_{int} is the focus of the bonding analysis. The interaction energy ΔE_{int} can be divided into three main components:

$$\Delta E_{int} = \Delta E_{elstat} + \Delta E_{pauli} + \Delta E_{orb}$$

ΔE_{elstat} represents the electrostatic interaction energy between the fragments calculated with a frozen electron density distribution in the complex. ΔE_{pauli} represents the
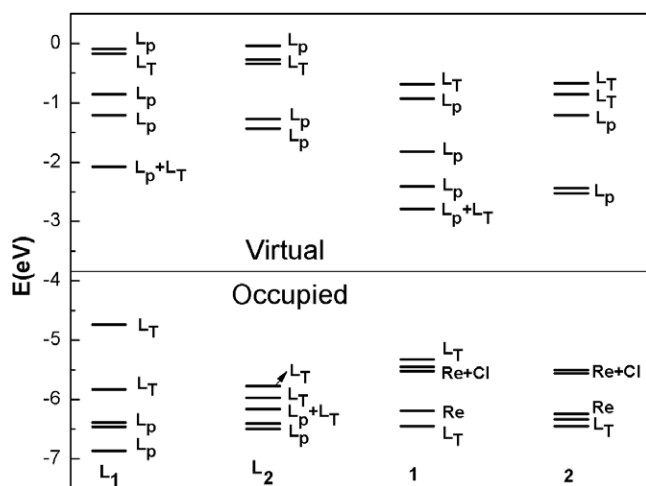

Fig. 2. Energy level diagram of frontier molecular orbitals of the two ligands and two complexes. (Labels on the right denote the dominant moiety contributing to each molecular orbital.)
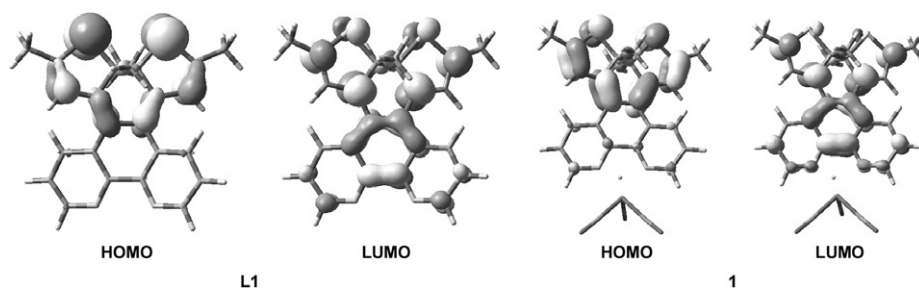

Fig. 3. Contour plots of highest occupied and lowest virtual orbitals in L_1 and **1**.

repulsive interactions between the fragments, which are caused by the fact that two electrons with the same spin cannot occupy the same region in space. The stabilizing orbital interaction term ΔE_{orb} is calculated in the final step of the EPA analysis when the Kohn–Sham orbitals relax to their form.

The results listed in Table 2 show that the electrostatic energy plays a more important role for the $Re(CO)_3Cl$-L binding than the orbital interaction, i.e., the Re–L interac-

tions have a larger electrostatic character than covalent character. Re–L interaction of **1** is larger than that of **2**, because orbital interaction makes **1** more stable than **2**. The more the electrons transfer from ligand (metal) to metal (ligand) for **1**, the larger the orbital interaction is (see Table 3). Furthermore, back donation of electrons from a 5d(Re) orbital of **1** into the empty π^*(ligand) orbital is about six times more than that of **2**, it is understandable because the energy of LUMO (empty π^*(ligand) orbital) is lower for **1**. It suggests that the back donation of electrons can be controlled by the π-conjugated length of ligand.

3.4. Photoexcitation

In order to observe the effects of the closed–open ring and metal complexation on excited-state properties of the title systems, TD-B3LYP calculations were performed to provide vertical transition energies from the ground-state geometries. The excited states of oscillator strength $f > 0.01$ were listed in Table 4.

An experimentally used model of an excited state corresponds to the excitation of an electron from an occupied MO to a virtual MO (i.e. a one-electron picture). However, the excited states calculated herein (TDDFT formulism) demonstrate that excited-state electronic structures are best described in terms of multiconfiguration, in which a linear combination of several occupied-to-virtual MO excitations comprises a given optical transition. Assignment of the

Table 2
Energy partitioning analysis of metal–ligand interaction in **1** and **2** at the level of BP86/TZP (ΔE/eV)

Term	**1**	**2**
ΔE_{int}	−3.335	−3.292
ΔE_{pauli}	7.741	7.752
ΔE_{elstat}	−6.949 (62.7%)	−6.960 (63.0%)
ΔE_{orb}	−4.128 (37.3%)	−4.084 (37.0%)

Table 3
Charge decomposition analysis of Re–N interaction in **1** and **2** at the level of B3LYP

Model complex	Donation	Back-donation
	L → Re	Re → L
1	0.559	0.065
2	0.504	0.016

Table 4
The absorption spectra (λ, nm), oscillator strengths (f), and dominant excitation character for singlet (S_n) and triplet (T_n)[a]

	λ_{calc}	f	Excitation[b]	State	Character	λ_{expt}
L_1	549.39	0.10	H → L (0.63)	$S_1(A)$	$L_T → L_T/L_P$ (IL, LLCT)	540
	356.83	0.31	H → L + 2 (0.54)	$S_4(A)$	$L_T → L_P$ (LLCT)	366
L_2	332.88	0.04	H → L (0.64)	$S_1(A)$	$L_T → L_P$ (LLCT)	
	295.93	0.07	H − 2 → L (0.57)	$S_7(A)$	$L_P/L_T → L_P$ (IL, LLCT)	300
1	592.56	0.06	H → L (0.54)	$S_1(A)$	$L_T → L_T/L_P$ (IL)	580
	590.80	0.02	H − 1 → L (0.54)	$S_2(A)$	$Re/Cl → L_T/L_P$ (MLCT/LLCT)	
	563.34	0.03	H − 2 → L (0.68)	$S_3(A)$	$Re/Cl → L_T/L_P$ (MLCT/LLCT)	
	493.88	0.03	H − 2 → L + 1 (0.66)	$S_6(A)$	$Re/Cl → L_P$ (MLCT/LLCT)	
	411.02	0.01	H − 1 → L + 2 (0.69)	$S_9(A)$	$Re/Cl → L_P$ (MLCT/LLCT)	
	386.74	0.44	H − 4 → L (0.48)	$S_{12}(A)$	$L_T → L_T/L_P$ (IL)	390
			H → L + 2 (0.41)		$L_T → L_P$ (IL)	
	365.06	0.02	H − 6 → L (0.62)	$S_{14}(A)$	$Re/Cl → L_T/L_P$ (MLCT/LLCT)	
2	559.15	0.00	H → L (0.70)	$S_1(A)$	$Re/Cl → L_P$ (MLCT/LLCT)	400
	525.14	0.03	H − 1 → L (0.62)	$S_2(A)$	$Re/Cl → L_P$ (MLCT/LLCT)	
	508.15	0.03	H → L + 1 (0.62)	$S_3(A)$	$Re/Cl → L_P$ (MLCT/LLCT)	
	380.26	0.02	H − 3 → L + 1 (0.60)	$S_8(A)$	$L_T → L_P$ (IL)	
	363.37	0.01	H − 4 → L (0.64)	$S_{10}(A)$	$L_T → L_P$ (IL)	
	349.15	0.05	H − 5 → L (0.61)	$S_{12}(A)$	$L_P/L_T/Re/Cl → L_P$ (IL, ML/LLCT)	
	333.13	0.03	H − 5 → L + 1 (0.57)	$S_{15}(A)$	$L_P/L_T/Re/Cl → L_P$ (IL, ML/LLCT)	
	331.94	0.05	H − 6 → L + 1 (0.49)	$S_{16}(A)$	$Re/Cl → L_P$ (MLCT/LLCT)	
			H − 1 → L + 2 (0.35)		$Re/Cl → L_P$ (MLCT/LLCT)	
	325.32	0.01	H − 7 → L (0.62)	$S_{17}(A)$	$L_T → L_P$ (IL)	
	321.80	0.02	H − 7 → L + 1 (0.65)	$S_{18}(A)$	$L_T → L_P$ (IL)	

[a] For L_1 and L_2, the thiophene moieties and 1,10-phenanthronline moiety are two different ligands, so the charge transfer between the two parts is defined as LLCT; but for **1** and **2**, both the thiophene moieties and 1,10-phenanthronline moiety belong to the same ligand, so the charge transfer between the two parts is defined as IL (H denotes the HOMO and L the LUMO.).
[b] The coefficient in the configuration interaction wave functions is given in parentheses in the column excitation.

character of each excited state is based on the compositions of the occupied and virtual MOs of the dominant configuration(s). Excited states originated from transitions between orbitals located on different moieties are classified as charge transfer (CT) excited states, such as metal-to-ligand charge transfer (MLCT) and ligand-to-ligand charge transfer (LLCT), but those from π-occupied to π-virtual orbitals located on the same ligand are described as intraligand (IL).

The $S_0 \rightarrow S_1$ excited states are mainly corresponding to the transition from HOMO to LUMO. According to the analysis in molecular orbitals, the transition character of L_1 and **1** is similar, which can be characterized as $\pi(L_T) \rightarrow \pi^*(L_T/L_P)$. For **1**, although not participating in transition orbitals, Re makes the spectrum shifted to long wavelength. There are two major reasons responsible for this shift: one is that the more LUMO and less HOMO levels of **1** are stabilized by Re(I) compared with L_1 (see Fig. 2); another is Re increases the coplanarity of ligand section, as mentioned above. Compared with L_1, the lowest transition energy of L_2 is blue shifted because of the shorter π-conjugated network.

The calculated results for L_1, L_2 and **1** agree well with the experimental determinations [6]. For **1**, the absorption band with the most significant oscillator strength at 386.74 nm arises from the $\pi(L_T) \rightarrow \pi^*(L_T/L_P)$ (IL) electronic transition of $S_{12}(A)$ allowed by selection rules, corresponding to the most intense absorption peak at 390 nm observed in experiments.

In the UV–Vis region, **2** has a moderately absorption at ca. 400 nm, which is typically observed in rhenium(I) tricarbonyl diimine complex systems [18,19], and thus is assigned as a MLCT $[d\pi(Re) \rightarrow \pi^*(L_P)]$ transition. However, Table 4 shows that the transition energy of the excited states characterized by MLCT deviates from the experimental result more than 50 nm. The solvent effect was taken into consideration to correct the deviation, but it was found that this effect leads to a little blue-shift in the MLCT excited states. Hence, we think that spin–orbit coupling (SOC) effects play an important role in MLCT excited states.

It should be pointed out that no spin–orbit interactions are included within the TDDFT results presented above. SOC causes the mixture of singlet and triplet states, the latter is allowed to participate in both absorption and emission. The two-component TDDFT (implemented in ADF) formalism is used here to evaluate the contributions to the excited states in terms of singlet and triplet single group scalar relativistic excited states. Besides the large size and no symmetry of the metal complexes considered here, the two-component TDDFT is very time-consuming method, so we just calculated the first 35 excited states to save computational effort. We just aim to gain insight into the effects of SOC on the excited states of heavy transition metal complexes by means of the two-component TDDFT.

The energy level and the constitution of FMO with and without SOC for **1** and **2** are listed in supporting information Tables S2 and S3. It can be seen that the components of FMOs in Table S2 and S3 are different from those in Table S1, which is reasonable because LB94 and B3LYP are used for the exchange and correlation (XC) functional, respectively. The former refers to the XC functional presented by Van Leeuwen and Baerends [20], and the latter refers to Becke's three-parameter hybrid method [21] using the Lee–Yang–Parr correlation functional [22].

From Table S2 and S3, it can be viewed that the spinors mainly composed of d(Re) mix significantly, leading to the spinor energies vary about 0.03–0.04 eV compared with the scalar orbital energies. But the components of the spinors are basically unchanged. SOC has negligible effect on the spinors characterized by π(ligand). From the above arguments, it can be concluded that the SOC effects on the excitation energies will mainly originate from the spin-orbit splitting of the 5d orbitals on Re. To check it, the selected excited states from two-component and scalar relativistic TDDFT calculations for **1** and **2** are listed in Table S4 (see the Supporting Information). The components of each double group excited state in terms of singlet and triplet single group excited states are also listed. Two points can be concluded from Table S4. One is that the transition out of π(ligand) orbital preserves the quality of its corresponding single group excited state, e.g., for the double excited state 24A of **1**, SOC will have tiny effect on this transition. The other is that although the states mainly characterized by MLCT mix significantly due to spin–orbital interactions, the main feature of the calculated spectra is about the same with or without SOC included. However, the transition energies are shifted around 0.05 eV compared with the single group excited states. Hence, although TDDFT (GAUSSIAN 03) cannot exactly estimate the excitation energies for the d(Re)-joined transitions, it can still provide available spectral feature for our title systems.

3.5. Photoluminescence

In general, for organic molecules, the fluorescence is dominant. However, for the complexes **1** and **2**, the spin–orbit effect is introduced due to the introduction of heavy metal. Especially, for the complex **2**, the main absorption spectra are characterized as MLCT. Hence, the contribution of phosphorescence should be considered. Moreover, TD-DFT calculated value (which is based on the ground state geometry) of S_1–T_1 energy gap of complex **2** (0.065 eV) is rather smaller than that of **1** (0.980 eV), which can lead to the effective intersystem crossing. Thus, the fluorescence signal is hardly detectable for **2**, and we just listed the triplet state of this compound in Table 5.

According to the empirical Kasha's rule [23], the luminescence of isolated systems commonly originates from the radiative decay of the lowest excited state. Thus, the photophysical properties of compounds are governed by their first singlet (S_1) and/or triplet (T_1) excited state. However, there may be an exception to this rule, such as in system **1**. Fig. 4 shows the energies of equilibrium

Table 5
Calculated TDDFT emission energies (nm) of the title systems with experimental data

	$\lambda_{calc.}$	f	State	Excitation[a]	Character	$\lambda_{expt.}$
L$_1$	641.29	0.10	S$_1$	L → H (0.61)	L$_P$/L$_T$ → L$_T$ (LLCT, IL)	644
L$_2$	363.32	0.16	S$_1$	L → H (0.61)	L$_P$ → L$_P$/L$_T$ (IL, LLCT)	385
1	2424.06	0.00	T$_1$	L + 1 → H (0.18)	L$_P$ → L$_T$ (IL)	
				L + 3 → H (0.16)	L$_P$ → L$_T$ (IL)	
	613.80	0.00	T$_2$	L + 2 → H (0.54)	L$_P$ → L$_T$ (IL)	620
	697.52	0.11	S$_1$	L → H (0.62)	L$_P$/L$_T$ → L$_T$ (IL)	
2	657.72	0.00	T$_1$	L → H − 3 (0.50)	L$_P$ → L$_T$ (IL)	595
				L → H − 1 (0.46)	L$_P$ → Re/Cl (LMCT/LLCT)	

[a] The coefficient in the configuration interaction wave functions is given in parentheses in the column excitation.
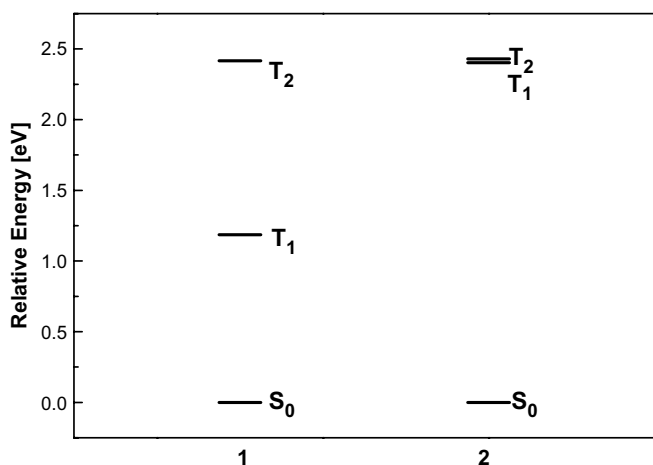

Fig. 4. Calculated energy levels of **1** and **2** at the same theory level (ab initio). (The relative ground-state S$_0$ is chosen as the reference point.)

geometries of S$_0$, T$_1$ and T$_2$ states for **1** and **2.** Note that a relatively large energy gap between T$_1$ and T$_2$ exists in **1**. Generally, a larger energy gap between the lowest and the next lowest excited-state tends to reduce the internal conversion and thus enhance the emission from the higher electronic state. Therefore, the second excited state (T$_2$) of **1** is also taken into account when interpreting the nature of luminescence.

For **1**, S$_0$–T$_1$ energy gap is 1.19 eV, which is lower than T$_1$–T$_2$ energy gap (1.23 eV). Thus, T$_2$ may contribute to the luminescence of **1** to some extent. According to our calculations, the T$_2$ of **1** is described by the L + 2 → H excitation and mainly corresponds to π^* (L$_P$) → π (L$_T$) (IL) transition (see Table 5). This excited state is predicted at 613.80 nm, which is in good agreement with the experimental data (620 nm). On the contrary, T$_2$ should not contribute to phosphorescence of **2** because of the quite smaller T$_1$–T$_2$ gap (0.03 eV). The T$_1$ of **2** is characterized as ILCT (π^* (L$_P$) → π (L$_T$)), LMCT and LLCT (π(L$_P$) → d(Re)/ p(Cl)). This excited state locates at 657.72 nm, which do not agree well with the experimental data (595 nm) because SOC effects are not included in the TDDFT results. SOC will have effects on the excited energy for the transition out of d(Re) in this systems, as stated above.

Table 5 shows the fluorescence of L$_1$ and L$_2$ consists of the transition from LUMO to HOMO. Compared with L$_2$, L$_1$ leads to a larger red shift because of the longer expanded π-conjugated network, which closely resembles those of the absorption maximum. In addition, similar to the case in the absorption spectrum, the coordination of Re makes the fluorescence of **1** shifted to long wavelength compared with L$_1$.

4. Conclusion

On the analysis of ground- and excited-state properties of the two ligands (L$_1$ and L$_2$) and two complexes [Re(CO)$_3$(L)Cl] (**1** and **2**), two points have been found. One is the effect of the metal complexation on the properties of excited states: (a) the incorporation of the metal center introduces more sublevels into the energy hierarchy, which allows complicated electronic transitions to occur; (b) simultaneously, spin–orbit coupling effect is also taken into consideration, and it influences the excitation energies for the d(Re)-joined transitions and has negligible effect on the transition character for this systems; (c) for the closed-ring complex **1**, the coordination of Re results in a little change in the transition character of the excited states with strongest oscillator strength and a red-shift in the transition energy. The other is the effect of closed–open ring on the properties of excited states: (a) compared with L$_2$, there is a red-shift in the absorption maximum and luminescent spectrum of the closed-ring ligand L$_1$ due to the longer π-conjugated network; (b) back donation of electrons from a 5d(Re) orbital of **1** into the empty π^*(ligand) is more than that of **2** because the longer π-conjugated network of ligand section decreases the energy of π^*(ligand), thus this metal–ligand interaction can be controlled by the extent of π-conjugation of ligand; (c) the transition character of the strongest absorption band and luminescent spectrum for closed-ring complex **1** is different from that of **2**, the former has $\pi\pi^*$ character and the latter has MLCT and LLCT character.

Appendix A. Supplementary material

Supplementary data associated with this article can be found, in the online version, at doi:10.1016/j.jorganchem.2007.08.031.

References

[1] (a) M. Irie, Chem. Rev. 100 (2000) 1683;
(b) M. Irie, Chem. Rev. 100 (2000) 1685;
(c) N. Tamai, H. Miyasaka, Chem. Rev. 100 (2000) 1875;
(d) C. Joachim, J.K. Gimzewski, A. Aviram, Nature 408 (2000) 541;
(e) F.M. Raymo, Adv. Mater. 14 (2002) 401;
(f) S.L. Gilat, S.H. Kawai, J.-M. Lehn, Chem. Eur. J. 1 (1995) 275;
(g) V. Balzani, A. Credi, M. Venturi, Chem. Phys. Chem. 4 (2003) 49;
(h) H. Tian, S.J. Yang, Chem. Soc. Rev. 33 (2004) 85.
[2] (a) H. Dürr, H. Bouas-Laurent (Eds.), Photochromism: Molecules and Systems, Elsevier, New York, 1990;
(b) J.C. Crano, R.J. Guglielmetti (Eds.), Organic Photochromic and Thermochromic Compounds, vol. 1, Plenum, New York, 1999.
[3] (a) T. Inada, S. Uchida, Y. Yokoyama, Chem. Lett. (1997) 321;
(b) Q.F. Luo, S.H. Sheng, S.H. Cheng, H. Tian, Aust. J. Chem. 58 (2005) 321.
[4] (a) H. Görner, C. Fischer, S. Gierisch, J. Daub, J. Phys. Chem. 97 (1993) 4110;
(b) J. Walz, K. Ulrich, H. Port, H.C. Wolf, J. Wonner, F. Effenberger, Chem. Phys. Lett. 213 (1993) 321;
(c) N.P.M. Huck, B.L. Feringa, J. Chem. Soc., Chem. Commun. (1995) 1095;
(d) G.M. Tsivgoulis, J.-M. Lehn, Angew. Chem., Int. Ed. Engl. 34 (1995) 1119.
[5] (a) H. Tian, S. Yang, Chem. Soc. Rev. 33 (2004) 85;
(b) M. Irie, O. Miyatake, K. Uchida, T. Eriguchi, J. Am. Chem. Soc. 116 (1994) 9894;
(c) T.B. Norsten, A. Peters, R. McDonald, M. Wang, N.R. Branda, J. Am. Chem. Soc. 123 (2001) 7447;
(d) E. Murguly, T.B. Norsten, N.R. Branda, Angew. Chem., Int. Ed. 40 (2001) 1752;
(e) A. Fernández-Acebes, J.M. Lehn, Adv. Mater. 10 (1998) 1519;
(f) H. Tian, B.Z. Chen, H. Tu, K. Müllen, Adv. Mater. 14 (2002) 918;
(g) R.T.F. Jukes, V. Adamo, F. Hartl, P. Belser, L. De Cola, Inorg. Chem. 43 (2004) 2779;
(h) A. Bianco, C. Bertarelli, J.F. Rabolt, G. Zerbi, Chem. Mater. 17 (2005) 869;
(i) Y.C. Jeong, S.I. Yang, K.H. Ahn, E. Kim, Chem. Commun. (2005) 2503;
(j) T.A. Golovkova, D.V. Kozlov, D.C. Neckers, J. Org. Chem. 70 (2005) 5545.
[6] V.W. Yam, C.C. Ko, N. Zhu, J. Am. Chem. Soc. 126 (2004) 12734.
[7] (a) W. Koch, M.C. Holthausen, A Chemist's Guide to Density Functional Theory, Wiley-VCH, Weinheim, Germany, 2000;
(b) C. Adamo, B.V. di Matteo, Adv. Quantum Chem. 36 (1999) 4.
[8] (a) J.B. Foresman, M. Head-Gordon, J.A. Pople, M.J. Frisch, J. Phys. Chem. 96 (1992) 135;
(b) J.B. Foresman, A.E. Frisch, Exploring Chemistry with Electronic Structure Methods, 2nd ed., Gaussian Inc., Pittsburgh, PA, 1995 (Chapter 8).
[9] (a) R. Bauernschmitt, R. Ahlrichs, Chem. Phys. Lett. 256 (1996) 454;
(b) M.K. Casida, C. Jamorski, K.C. Casida, D.R. Salahub, J. Chem. Phys. 108 (1998) 4439;
(c) N.N. Matsuzawa, A. Ishitani, T. Uda, J. Phys. Chem. A 105 (2001) 4953.
[10] M.J. Frisch, G.W. Trucks, H.B. Schlegel, G.E. Scuseria, M.A. Robb, J.R. Cheeseman, J.A. Montgomery Jr., T. Vreven, K.N. Kudin, J.C. Burant, J.M. Millam, S.S. Iyengar, J. Tomasi, V. Barone, B. Mennucci, M. Cossi, G. Scalmani, N. Rega, G.A. Petersson, H. Nakatsuji, M. Hada, M. Ehara, K. Toyota, R. Fukuda, J. Hasegawa, M. Ishida, T. Nakajima, Y. Honda, O. Kitao, H. Nakai, M. Klene, X. Li, J.E. Knox, H.P. Hratchian, J.B. Cross, C. Adamo, J. Jaramillo, R. Gomperts, R.E. Stratmann, O. Yazyev, A.J. Austin, R. Cammi, C. Pomelli, J.W. Ochterski, P.Y. Ayala, K. Morokuma, G.A. Voth, P. Salvador, J.J. Dannenberg, V.G. Zakrzewski, S. Dapprich, A.D. Daniels, M.C. Strain, O. Farkas, D.K. Malick, A.D. Rabuck, K. Raghavachari, J.B. Foresman, J.V. Ortiz, Q. Cui, A.G. Baboul, S. Clifford, J. Cioslowski, B.B. Stefanov, G. Liu, A. Liashenko, P. Piskorz, I. Komaromi, R.L. Martin, D.J. Fox, T. Keith, M.A. Al-Laham, C.Y. Peng, A. Nanayakkara, M. Challacombe, P.M.W. Gill, B. Johnson, W. Chen, M.W. Wong, C. Gonzalez, J.A. Pople, GAUSSIAN 03, revision C.02; Gaussian, Inc., Wallingford, CT, 2004.
[11] (a) F. Wang, T. Ziegler, J. Chem. Phys. 122 (2005) 204103;
(b) F. Wang, T. Ziegler, J. Chem. Phys. 123 (2005) 194102.
[12] (a) G. te Velde, S.J.A. Bickelhaupt, V. Gisbergen, C. Fonseca Guerra, E.J. Baerends, J.G. Snijders, T. Ziegler, J. Comput. Chem. 22 (2001) 931;
(b) C.F. Guerra, J.G. Snijders, G. te Velde, E.J. Baerends, Theor. Chem. Acc. 99 (1998) 391;
(c) ADF2006.01, SCM, Theoretical Chemistry, Vrije Universiteit, Amsterdam, The Netherlands, <http://www.scm.com>.
[13] (a) S.I. Gorelsky, AOMix: Program for Molecular Orbital Analysis, York University, Toronto, 1997. <http://www.sg-chem.net/>;
(b) S.I. Gorelsky, A.B.P. Lever, J. Organomet. Chem. 635 (2001) 187.
[14] C. Adamo, V. Bareone, Theo. Chem. Acc. 105 (2000) 169.
[15] K.J. Morokuma, Chem. Phys. 55 (1971) 1236.
[16] T. Ziegler, A. Rauk, Theor. Chim. Acta 46 (1977) 1.
[17] (a) S. Dapprich, G. Frenking, J. Phys. Chem. 99 (1995) 9352;
(b) G. Frenking, N. Frohlich, Chem. Rev. 100 (2000) 717.
[18] D.J. Stufkens, A. Vlček Jr., Coord. Chem. Rev. 177 (1998) 127.
[19] H.A. Nieawenhuis, D.J. Stufkens, J. Derk, J. Am. Chem. Soc. 117 (1995) 5579.
[20] R. van Leeuwen, E.J. Baerends, Physical Review A 49 (1994) 2421.
[21] A.D. Becke, J. Chem. Phys. 98 (1993) 5648.
[22] (a) A.D. Becke, J. Chem. Phys. 98 (1993) 5648;
(b) A.D. Becke, J. Chem. Phys. 98 (1993) 5648.
[23] (a) A.D. Becke, J. Chem. Phys. 98 (1993) 5648;
(b) A.D. Becke, J. Chem. Phys. 98 (1993) 5648.